

# Unravelling Complex Spectra of a Simple Molecule: REMPI Study of the 420 nm Band System of KRb\*\*

Yonghoon Lee,<sup>[b]</sup> Youngjee Yoon,<sup>[a, e]</sup> Jin-Tae Kim,<sup>[c]</sup> Sungyul Lee,<sup>\*,[d]</sup> and Bongsoo Kim<sup>\*,[a]</sup>

*This article is dedicated to Prof. Karl Kleinermanns on the occasion of his 60th birthday*

Complex spectra of the KRb 420 nm system are analyzed by mass-resolved resonance enhanced two-photon ionization in a cold molecular beam. Vibronic structures of three singlet–singlet ( $4^1\Pi$ ,  $7^1\Sigma^+$ , and  $5^1\Pi \leftarrow X^1\Sigma^+$ ) transitions were identified for the first time. By comparing with highly accurate ab initio

calculations, we assigned the singlet excited electronic states, and determined their electronic term values and vibrational constants. Weak singlet–triplet transitions were observed and identified as the  $5^3\Pi(0^+) \leftarrow X^1\Sigma^+$  transitions by the homogeneous perturbation selection rule.

## 1. Introduction

A diatomic molecule is the simplest form of a molecule. Alkali metal diatomic molecules consist of two alkali group elements and have only two valence electrons. In spite of their simple structures, their high density of electronic states in the high energy region,<sup>[1–12]</sup> their complex interactions,<sup>[13–24]</sup> and contributions from several isotopomers of alkali dimers make their excitation spectra extremely complex, and the interpretation of the spectra becomes quite challenging. Fortunately, the small numbers of nuclei and valence electrons enable accurate prediction of electronic structures of alkali dimers by ab initio calculations.<sup>[1–12]</sup> For KRb, electronic term values,  $T_e$ , and equilibrium internuclear distances,  $R_e$ , have been predicted by theory with errors less than 1%.<sup>[8]</sup> For RbCs and Rb<sub>2</sub>, the predicted values show errors less than 2%.<sup>[7,9]</sup> These highly accurate theoretical calculations of the excited-state molecular parameters help us to interpret their complex spectra and obtain accurate spectroscopic information on their highly excited electronic states.

Mass-resolved resonance-enhanced multi-photon ionization (REMPI) in a very cold molecular beam has greatly simplified the complex excitation spectra of alkali dimers overlapped by contributions from several isotopomers by extensive cooling in a pulsed molecular beam and separating the contributions from individual isotopomers.<sup>[13–18]</sup> The vibrational quantum numbers ( $v'$ ) of excited levels can be conveniently and accurately assigned by spectra from different isotopomers.<sup>[25]</sup> In addition, most of the excited states of alkali dimers can be reached by visible light and absorbing another photon with the same wavelength easily ionizes the alkali molecules, enabling the mass-separated detection. Since the spectroscopy of KRb as of 2010 is summarized in our recent paper,<sup>[26]</sup> it will not be detailed here.

Herein, we have investigated complex vibronic structures of KRb near 420 nm by mass-resolved resonance-enhanced two-photon ionization (REMPI) in a cold molecular beam. The  $4^1\Pi$   $v'=4$ –27,  $7^1\Sigma^+$   $v'=5$ –23, and  $5^1\Pi$   $v'=4$ –30  $\leftarrow X^1\Sigma^+$   $v''=0$  transitions have been observed and identified for the first

time. These singlet excited electronic states are the highest-lying electronic states of KRb observed so far. The experimentally determined  $T_e$  values and vibrational constants of the excited electronic states agree very well with those from ab initio calculations.<sup>[8]</sup> We also identified the  $5^3\Pi(0^+) \leftarrow X^1\Sigma^+$  transition that probably borrows transition intensities from the  $7^1\Sigma^+ \leftarrow X^1\Sigma^+$  transition by homogeneous perturbation, causing anomalous behavior of vibrational spacing in the  $7^1\Sigma^+$  state.

## 2. Results and Discussion

### 2.1. Main Bands: $4^1\Pi$ , $7^1\Sigma^+$ , and $5^1\Pi \leftarrow X^1\Sigma^+$

Figure 1 shows the REMPI spectra recorded at the channels of  $m/z$  124 ( $^{39}\text{K}^{85}\text{Rb}$ ) and 126 ( $^{39}\text{K}^{87}\text{Rb}$  and  $^{41}\text{K}^{85}\text{Rb}$ ) between 23 100 and 24 870  $\text{cm}^{-1}$ . Three strong vibrational progressions were identified and denoted as  $\alpha$ ,  $\beta$ , and  $\gamma$  bands with the deter-

[a] Dr. Y. Yoon, Prof. B. Kim  
Department of Chemistry, KAIST  
Daejeon 305-701 (Korea)  
Fax: (+82) 42-350-2810  
E-mail: bongsoo@kaist.ac.kr

[b] Prof. Y. Lee  
Department of Chemistry, Mokpo National University  
Muan-gun, Jeonnam 534-729 (Korea)

[c] Prof. J. T. Kim  
Department of Photonic Engineering, Chosun University  
Gwangju 501-759 (Korea)

[d] Prof. S. Lee  
Department of Applied Chemistry, Kyung Hee University  
Gyeonggi-do 449-701 (Korea)  
Fax: (+82) 31-202-7337  
E-mail: syllee@khu.ac.kr

[e] Dr. Y. Yoon  
Memory Division, Samsung Electronics Co., Ltd.  
Hwasung, Gyeonggi-do 445-701 (Korea)

[\*\*] REMPI: Resonance-Enhanced Multi-Photon Ionization

Supporting information for this article is available on the WWW under <http://dx.doi.org/10.1002/cphc.201000989>.

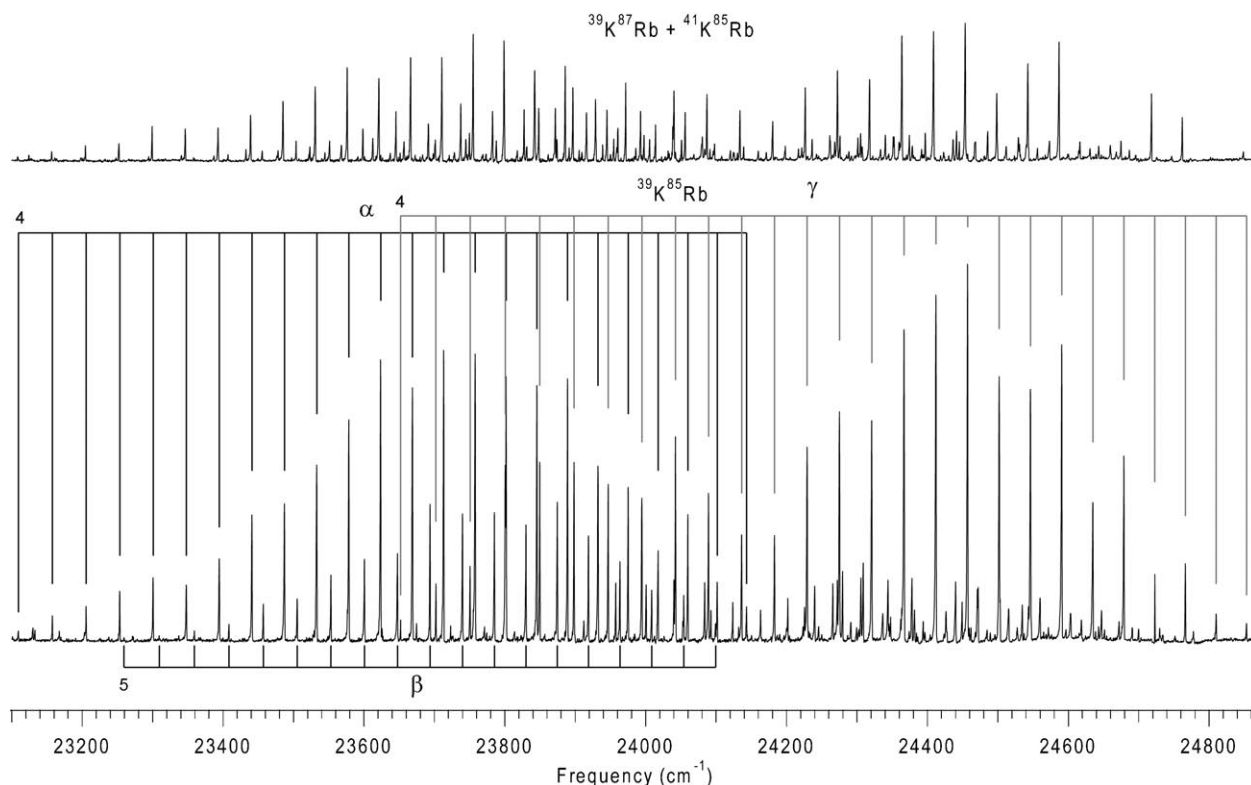


**Figure 1.** RE2PI spectra recorded at the channels of  $m/z$  124 ( $^{39}\text{K}^{85}\text{Rb}$ ) and 126 ( $^{39}\text{K}^{87}\text{Rb}$  and  $^{41}\text{K}^{85}\text{Rb}$ ) between 23 100 and 24 870  $\text{cm}^{-1}$  obtained by Kr carrier gas. The three strong vibrational progressions are denoted as  $\alpha$ ,  $\beta$ , and  $\gamma$ . The  $v'$  numbers of the lowest-lying  $\alpha$ ,  $\beta$ , and  $\gamma$  bands are given.

mined  $v'$  numbers. The vibrational term values,  $T_v$  (=band origin +  $G_{v'=0}$ ), of  $^{39}\text{K}^{85}\text{Rb}$ ,  $^{39}\text{K}^{87}\text{Rb}$ , and  $^{41}\text{K}^{85}\text{Rb}$  for the  $\alpha$ ,  $\beta$ , and  $\gamma$  bands are listed in the Supporting Information. The intensity distribution of the observed vibronic bands showing two maxima with a minimum near 24 160  $\text{cm}^{-1}$  is due to the characteristic efficiency spectrum of the laser dye (Exalite 428, Exciton, Inc.) used in the experiment.<sup>[27]</sup>

The lower vibronic levels for the observed transitions are identified by the difference between hot ( $v' \leftarrow v''=1$ ) and origin ( $v' \leftarrow v''=0$ ) band positions with a common upper ( $v'$ ) level. This is equal to the energy difference between the  $v''=1$  and 0 levels of the  $X^1\Sigma^+$  state,  $G_{v''=1} - G_{v''=0}$ .<sup>[28]</sup> Thus, under our experimental conditions, most KRb molecules were found to be in the  $X^1\Sigma^+$   $v''=0$  level. See the Supporting Information for assignments of the  $v'=15-30 \leftarrow v''=0$  and  $v'=17-30 \leftarrow v''=1$  transitions of  $\gamma$  bands.

Figure 2 shows the nonrelativistic ab initio potential energy curves (PECs) of the excited electronic states near the observed spectral region.<sup>[8]</sup> The vertical dotted line represents the Franck–Condon (FC) excitation from the  $X^1\Sigma^+$   $v''=0$  level. (A color version of Figure 2 is given in the Supporting Information.) Three singlet states,  $4^1\Pi$ ,  $7^1\Sigma^+$ , and  $5^1\Pi$ , are predicted to be observed in the KRb 420 nm band system. Additionally, three triplet excited electronic states,  $6^3\Sigma^+$ ,  $5^3\Pi$ , and  $2^3\Delta$ , are located in the FC region and  $7^3\Sigma^+$  is located out of the FC region. The PEC crossings between the singlet and triplet states ( $5^1\Pi-7^3\Sigma^+$ ,  $5^1\Pi-2^3\Delta$ , and  $7^1\Sigma^+-5^3\Pi$  around 5.2, 5.8, and 4.0 Å, respectively) are predicted in Hund's case (a). As-

signing the upper states of the main  $\alpha$ ,  $\beta$ , and  $\gamma$  bands to the three singlet excited electronic states and those of the extra bands observed above 23 900  $\text{cm}^{-1}$  to the triplet excited elec-

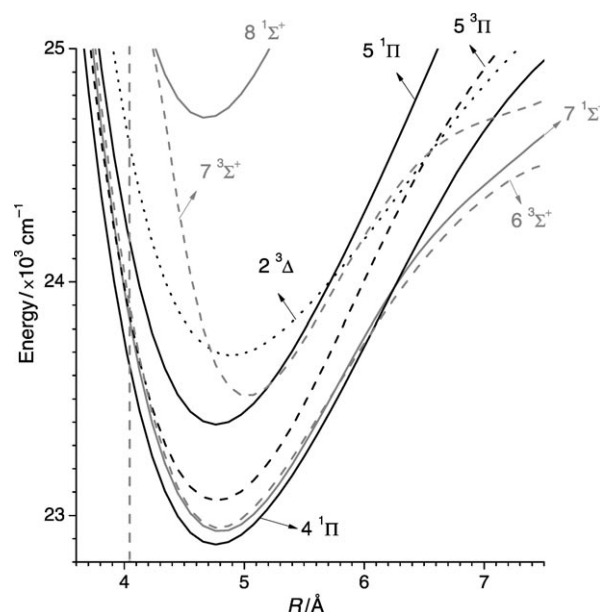


**Figure 2.** Nonrelativistic ab initio PECs of KRb for the singlet and triplet excited electronic states of the 420 nm band system. The vertical dotted line represents the FC region ( $R_e$  of the  $X^1\Sigma^+$  state, 4.055 Å, from ref. [8]). The origin of the ordinate axis is set to the potential minimum of the  $X^1\Sigma^+$  state.

tronic states seems to be a reasonable starting point for the extensive analysis of these complex spectra.

The vertical transition energy of the  $5^1\Pi \leftarrow X^1\Sigma^+$  transition is much higher than those of  $4^1\Pi$  and  $7^1\Sigma^+ \leftarrow X^1\Sigma^+$  transitions (Figure 2). Figure 3 compares the calculated FC factors,  $|\langle v' | v''=0 \rangle|^2$ , of the  $4^1\Pi$ ,  $7^1\Sigma^+$ , and  $5^1\Pi$   $v' \leftarrow X^1\Sigma^+$   $v''=0$  transitions and the observed vibronic band intensity distributions of  $\alpha$ ,  $\beta$ , and  $\gamma$  bands. The FC factors were calculated using the ab initio PECs of the  $4^1\Pi$ ,  $7^1\Sigma^+$ ,  $5^1\Pi$  and  $X^1\Sigma^+$  states from ref. [8] and the LEVEL 7.7 program.<sup>[29]</sup> The observed band intensities in Figure 3a–c were divided by the laser dye efficiency for power normalization.

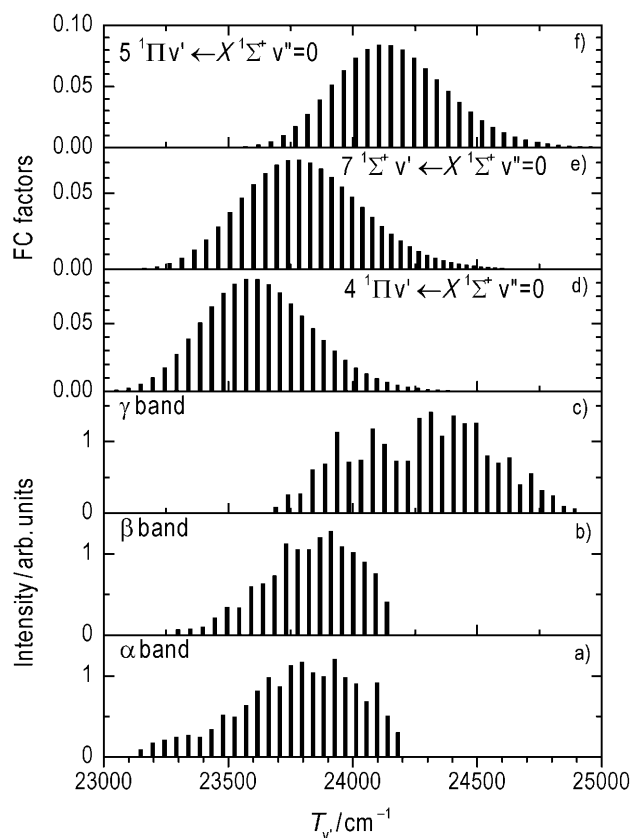


**Figure 3.** Observed vibronic-band intensity distributions of a)  $\alpha$  bands, b)  $\beta$  bands, and c)  $\gamma$  bands are compared with FC factors,  $|\langle v' | v''=0 \rangle|^2$ , of d)  $4^1\Pi$ , e)  $7^1\Sigma^+$ , and f)  $5^1\Pi \leftarrow X^1\Sigma^+$  transitions calculated using the ab initio PECs taken from ref. [8]. In order to correct the effect of the laser dye efficiency on the band intensities, the observed band intensities were divided by the laser dye efficiency (ref. [27]). The maximum of the intensity distribution of the  $\gamma$  bands is located higher in energy than those of the  $\alpha$  and  $\beta$  bands.

Comparing the intensity distributions of  $\alpha$ ,  $\beta$ , and  $\gamma$  bands with the calculated FC factors leads us to assign the upper electronic state of  $\gamma$  bands to the  $5^1\Pi$  state. Since the corrected intensity distribution maximum of the  $\gamma$  bands is located higher in energy than those of the  $\alpha$  and  $\beta$  bands, this assignment of the  $\gamma$  bands becomes clear, although the upper electronic states for the  $\alpha$  and  $\beta$  bands cannot be identified clearly to be the  $4^1\Pi$  or  $7^1\Sigma^+$  states by this comparison.

The  $v'$  numbers as well as the upper electronic states of these main bands can be assigned by comparing the experimental  $T_e$  values and harmonic vibrational constants,  $\omega_e$ , with the theoretical ones. The  $v'$  numbers of the  $\alpha$ ,  $\beta$ , and  $\gamma$  bands were determined by isotopomer shifts of upper vibrational levels as follows. In Figure 4, the observed isotope shifts,  $\Delta T_v$ ,

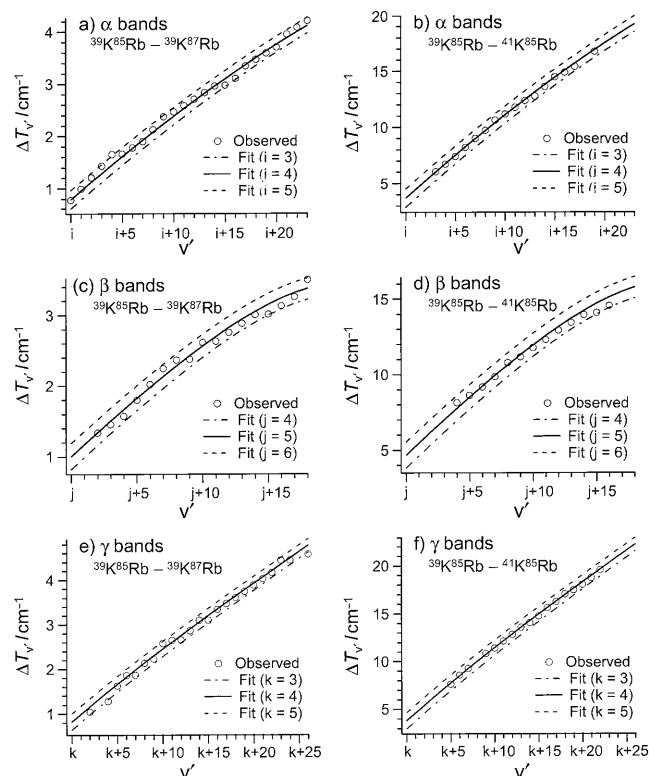


**Figure 4.** Comparison of observed and expected isotope shift values of  $\alpha$  [ $T_v(^{39}\text{K}^{85}\text{Rb}) - T_v(^{39}\text{K}^{87}\text{Rb})$  in (a) and  $T_v(^{39}\text{K}^{85}\text{Rb}) - T_v(^{41}\text{K}^{85}\text{Rb})$  in (b)],  $\beta$  [ $T_v(^{39}\text{K}^{85}\text{Rb}) - T_v(^{39}\text{K}^{87}\text{Rb})$  in (c) and  $T_v(^{39}\text{K}^{85}\text{Rb}) - T_v(^{41}\text{K}^{85}\text{Rb})$  in (d)], and  $\gamma$  [ $T_v(^{39}\text{K}^{85}\text{Rb}) - T_v(^{39}\text{K}^{87}\text{Rb})$  in (e) and  $T_v(^{39}\text{K}^{85}\text{Rb}) - T_v(^{41}\text{K}^{85}\text{Rb})$  in (f)] bands. The expected values were calculated for the three most possible assignments of  $v'$  numbers.

[ $=T_v(^{39}\text{K}^{85}\text{Rb}) - T_v(^{39}\text{K}^{87}\text{Rb})$  and  $T_v(^{39}\text{K}^{85}\text{Rb}) - T_v(^{41}\text{K}^{85}\text{Rb})$ ] of  $\alpha$ ,  $\beta$ , and  $\gamma$  bands are compared with three sets of the calculated values from the fitted molecular constants. The observed  $T_v$  values of the three isotopomers are simultaneously fitted to the following mass-reduced equation [Eq. (1)]:<sup>[25]</sup>

$$T_v = T_e + \omega_e \rho (v' + 1/2) - \omega_e x_e [\rho (v' + 1/2)]^2 + \omega_e y_e [\rho (v' + 1/2)]^3 + \omega_e z_e [\rho (v' + 1/2)]^4 + \dots \quad (1)$$

The constant  $\rho$  is 0.996378990 for  $^{39}\text{K}^{87}\text{Rb}$  and 0.983139464 for  $^{41}\text{K}^{85}\text{Rb}$ . Prior to fitting the  $T_v$  data set of three isotopomers to the above mass-reduced equation, the  $v'$  numbers should be assigned. For  $\alpha$  and  $\beta$  bands, high-order anharmonic vibrational constants up to  $\omega_e z_e$  were included in the fits. For the vibrational fit of  $\gamma$  bands, high-order constants up to  $\omega_e y_e$  were effective. Then, the  $\Delta T_v$  values were calculated using the following equation [Eq. (2)]:<sup>[25]</sup>

$$\begin{aligned}\Delta T_v = & \omega_e(v' + 1/2) - \omega_e x_e(v' + 1/2)^2 + \omega_e y_e(v' + 1/2)^3 + \\ & \omega_e z_e(v' + 1/2)^4 + \dots - \{ \omega_e \rho(v' + 1/2) - \\ & \omega_e x_e[\rho(v' + 1/2)]^2 + \omega_e y_e[\rho(v' + 1/2)]^3 + \\ & \omega_e z_e[\rho(v' + 1/2)]^4 + \dots \}\end{aligned}\quad (2)$$

The  $v'$  numbers of the lowest-lying  $\alpha$ ,  $\beta$ , and  $\gamma$  bands,  $i$ ,  $j$ , and  $k$ , are assigned to 4, 5, and 4, respectively. These assignments provide the best agreement between the calculated  $\Delta T_v$  values and the observed ones (see Figure 4).

The assignments and experimentally determined molecular constants are summarized and compared with theoretical values in Table 1. Figure 5 compares the experimental  $T_e$  and  $\omega_e$  values with theoretical ones. Considering the expected

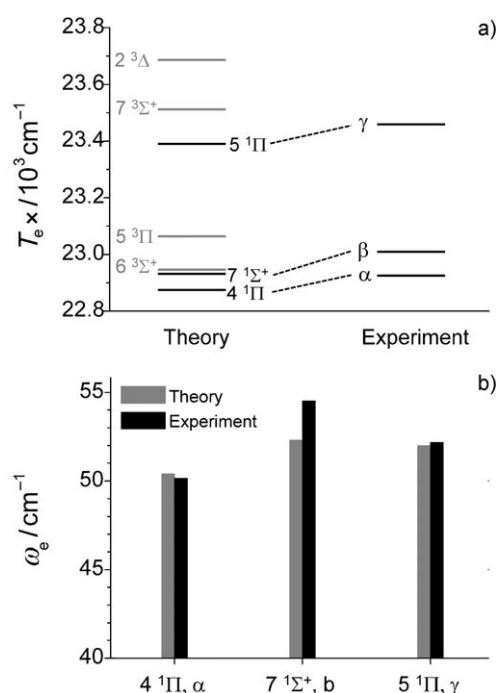


**Figure 5.** Comparison of a) electronic term value ( $T_e$ ) and b) harmonic vibrational frequency ( $\omega_e$ ) between our experiment and theory (ref. [8]). Assignments of the upper electronic states of  $\alpha$ ,  $\beta$ , and  $\gamma$  bands to the  $4^1\Pi$ ,  $7^1\Sigma^+$ , and  $5^1\Pi$  states are indicated by the dotted lines in (a).

error of the theoretical values being less than 1% for  $T_e$  and less than 10% for  $\omega_e$ ,<sup>[8]</sup> the upper electronic states of the  $\alpha$ ,  $\beta$ , and  $\gamma$  bands could be assigned to the  $4^1\Pi$ ,  $7^1\Sigma^+$ , and  $5^1\Pi$  states as indicated by the dotted lines in Figure 5a.

## 2.2. Extra Bands: $5^3\Pi(0^+) \leftarrow X^1\Sigma^+$

In Figure 1 several extra bands were observed above  $23900 \text{ cm}^{-1}$ . These weak vibronic structures can be attributed to the results of perturbation between the singlet ( $4^1\Pi$ ,  $5^1\Pi$ , and  $7^1\Sigma^+$ ) and triplet ( $6^3\Sigma^+$ ,  $5^3\Pi$ ,  $7^3\Sigma^+$ , and  $2^3\Delta$ ) excited electronic states located in this energy region. Figure 6 shows the experimentally observed vibrational spacings,  $\Delta G_v (=G_{v+1} - G_v)$  of the  $\alpha$  ( $4^1\Pi$ ),  $\beta$  ( $7^1\Sigma^+$ ), and  $\gamma$  ( $5^1\Pi$ ) bands and the corresponding theoretical values from the ab initio  $4^1\Pi$ ,  $7^1\Sigma^+$ , and  $5^1\Pi$  PECs (ref. [8]). Since the three  $\Delta G_v$  curves of these main bands show smooth and slowly changing shape and also the intensities of the extra bands are considerably weaker than those of the main bands (Figure 1), the singlet–

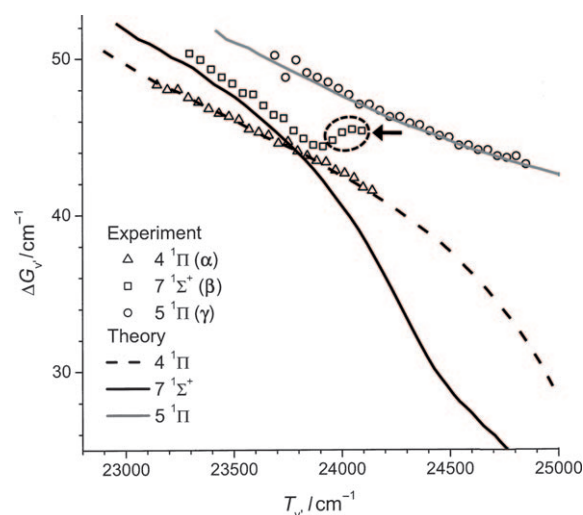


**Figure 6.** Experimentally observed vibrational spacings and the corresponding values calculated using the ab initio PECs taken from ref. [8]. For the  $7^1\Sigma^+$  state, the unexpected behavior of vibrational spacing is indicated by an arrow.

**Table 1.** Experimental<sup>[a]</sup> and theoretical<sup>[b]</sup> molecular constants of the KRb  $4^1\Pi$ ,  $7^1\Sigma^+$ ,  $5^1\Pi$ ,  $6^3\Sigma^+$ ,  $7^3\Sigma^+$ ,  $5^3\Pi$ , and  $2^3\Delta$  states.

	$T_e$ [ $\text{cm}^{-1}$ ]	$\omega_e$ [ $\text{cm}^{-1}$ ]	$\omega_e x_e$ [ $\text{cm}^{-1}$ ]	$\omega_e y_e$ [ $\text{cm}^{-1}$ ]	$\omega_e z_e$ [ $\text{cm}^{-1}$ ]	$R_e$ [ $\text{\AA}$ ]
$\alpha$ [ $4^1\Pi$ ] <sup>[a]</sup>	22925.30(53)	50.15(17)	0.195(18)	0.00215(82)	−0.000036(13)	
$\beta$ [ $7^1\Sigma^+$ ] <sup>[a]</sup>	23009.3(22)	54.51(83)	0.47(11)	0.0149(63)	−0.00034(13)	
$\gamma$ [ $5^1\Pi$ ] <sup>[a]</sup>	23459.09(29)	52.171(58)	0.2199(35)	0.001597(65)		
$7^1\Sigma^+$ <sup>[b]</sup>	22932	52.3				4.803
$4^1\Pi$ <sup>[b]</sup>	22875	50.4				4.763
$5^1\Pi$ <sup>[b]</sup>	23390	52.0				4.767
$6^3\Sigma^+$ <sup>[b]</sup>	22946	55.5				4.787
$7^3\Sigma^+$ <sup>[b]</sup>	23512	62.7				5.022
$5^3\Pi$ <sup>[b]</sup>	23064	51.8				4.774
$2^3\Delta$ <sup>[b]</sup>	23686	43.4				4.890

[a] This work. [b] Ref. [8].

triplet mixing does not seem to be very strong.

Note that the vibrational spacing of the five highest-lying  $\beta$  bands abnormally increases with  $v'$  (indicated by the arrow in Figure 6). Upon close inspection of the expanded RE2PI spectrum of  $^{39}\text{K}^{85}\text{Rb}$  around  $24000 \text{ cm}^{-1}$  in Figure 7, we find another vibrational progression denoted as  $\delta$ . The positions of  $\delta$  bands of  $^{39}\text{K}^{85}\text{Rb}$  and  $^{39}\text{K}^{87}\text{Rb}$  are listed in the Supporting Informa-

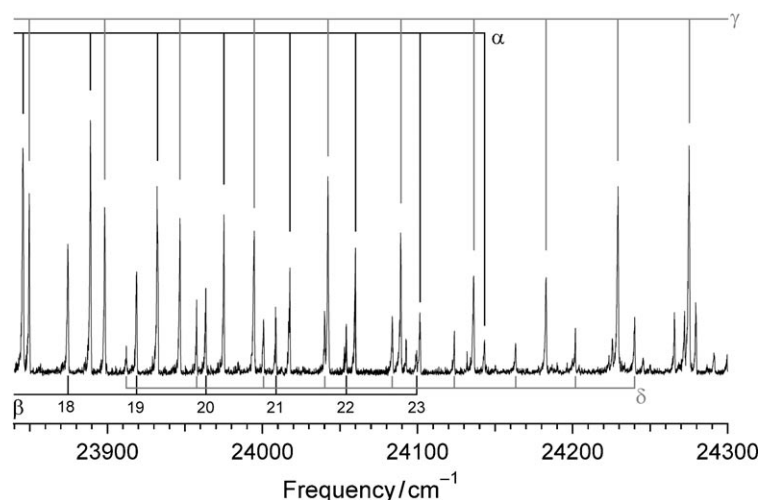


**Figure 7.** Expanded RE2PI spectrum of  $^{39}\text{K}^{85}\text{Rb}$  between 23840 and 24300  $\text{cm}^{-1}$ . The extra bands are denoted as  $\delta$ . The  $v'$  values of the  $\beta$  bands are given.

tion. We suggest the assignment of these  $\delta$  bands around 24080  $\text{cm}^{-1}$  to the  $5^3\Pi(0^+)$   $v' \leftarrow X^1\Sigma^+ v'' = 0$  transition. The five lowest-lying  $\delta$  bands lie close to the red side of the five highest-lying  $\beta$  bands,  $\Delta G_v$  values of which are abnormal. The abnormal increase in the  $\Delta G_v$  values of the five highest-lying  $\beta$  vibronic bands indicates the possibility of perturbation and/or an avoided crossing.

As mentioned above, there are four triplet excited electronic states in this energy region; the  $6^3\Sigma^+$ ,  $5^3\Pi$ ,  $7^3\Sigma^+$ , and  $2^3\Delta$  states (Figure 2). From the selection rule of homogeneous perturbation ( $\Delta\Omega = 0$  with  $\Delta J = 0$  and  $\Omega = \Lambda + \Sigma$ ), only the  $\Omega = 0^+$  component of the  $5^3\Pi$  state can perturb the  $7^1\Sigma^+$  state.<sup>[30]</sup> Because the  $\Omega$  substate,  $0^+$ , can only originate from the  $5^3\Pi$  state in this energy region ( $0^+$ , 1, and 2 from  $5^3\Pi$ ;  $0^-$  and 1 from  $6^3\Sigma^+$  and  $7^3\Sigma^+$ ; 1, 2, and 3 from  $2^3\Delta$ ), we assign the final state of the  $\delta$  bands to the  $5^3\Pi(0^+)$  state. Figure 8 compares the observed isotope shift,  $\Delta T_v [= T_v(^{39}\text{K}^{85}\text{Rb}) - T_v(^{39}\text{K}^{87}\text{Rb})]$  and  $\Delta G_v$  values of  $\delta$  bands with those from the  $6^3\Sigma^+$ ,  $5^3\Pi$ ,  $7^3\Sigma^+$ , and  $2^3\Delta$  ab initio PECs.<sup>[8]</sup> The  $\Delta T_v$  values of the  $\delta$  bands agree well with those from the ab initio  $5^3\Pi$  PEC. The  $\Delta G_v$  values of the  $\delta$  bands show some deviation from the calculated values due to perturbation by the  $7^1\Sigma^+$  state. The abnormal increase in the  $\Delta G_v$  values in the region of the  $7^1\Sigma^+$   $v' = 19$ –23 levels (around 24050  $\text{cm}^{-1}$ ) suggests an avoided crossing between the  $7^1\Sigma^+$  and  $5^3\Pi$  states [in Hund's case (c)].

Ab initio calculation predicts that the inner walls of the  $7^1\Sigma^+$  and  $5^3\Pi$  PECs cross each other at 24068  $\text{cm}^{-1}$  assuming Hund's case (a) [see the Supporting Information].<sup>[8]</sup>

### 3. Conclusions

We have identified three singlet excited electronic states,  $4^1\Pi$ ,  $7^1\Sigma^+$ , and  $5^1\Pi$ , in the KRB 420 nm band system by mass-resolved RE2PI in a cold molecular beam. The electronic term values and vibrational constants were determined. Anomalous  $\Delta G_v$  values of the  $7^1\Sigma^+$   $v' = 19$ –23 levels suggest an avoided

crossing with a nearby state. The homogeneous perturbation selection rule identifies the perturbing triplet state as the  $5^3\Pi(0^+)$  state.

### Experimental Section

The experimental details have been described previously.<sup>[14,26]</sup> In brief, KRB was formed by expanding K and Rb vapour with Kr carrier gas through a home-made high-temperature pulsed nozzle with an 800  $\mu\text{m}$  diameter orifice. The alkali metal sample was heated to 300  $^\circ\text{C}$ . The mixture of alkali metal vapour and Kr gas expanded into a high-vacuum chamber. The pulsed jet was collimated by a 1.2 mm diameter skimmer. In the collimated molecular beam,  $^{39}\text{K}^{85}\text{Rb}$  (67.3%),  $^{39}\text{K}^{87}\text{Rb}$  (26.0%),  $^{41}\text{K}^{85}\text{Rb}$  (4.9%), and  $^{41}\text{K}^{87}\text{Rb}$  (1.9%) isotopomers are formed. The molecular beam was intersected by a Nd:YAG pumped dye laser beam. Exciting the Exalite 428 dye solution by a third harmonic of a Nd:YAG laser, we obtained wavelength tunability between 399 and 436 nm. Two photons from the dye laser excited and ionized KRB isotopomers in the molecular beam. The ionized KRB isotopomers were mass-separated and detected by a linear time-of-flight (TOF) mass spectrometer ( $m/\Delta m \approx 500$ ) with a micro-channel plate detector. The ion signals were gated at the mass-to-charge ratios,  $m/z$  124 ( $^{39}\text{K}^{85}\text{Rb}^+$ ) and 126 ( $^{39}\text{K}^{87}\text{Rb}^+$  and  $^{41}\text{K}^{85}\text{Rb}^+$ ). Although the mass spectra of  $^{39}\text{K}^{87}\text{Rb}^+$  and  $^{41}\text{K}^{85}\text{Rb}^+$  could not be separated,

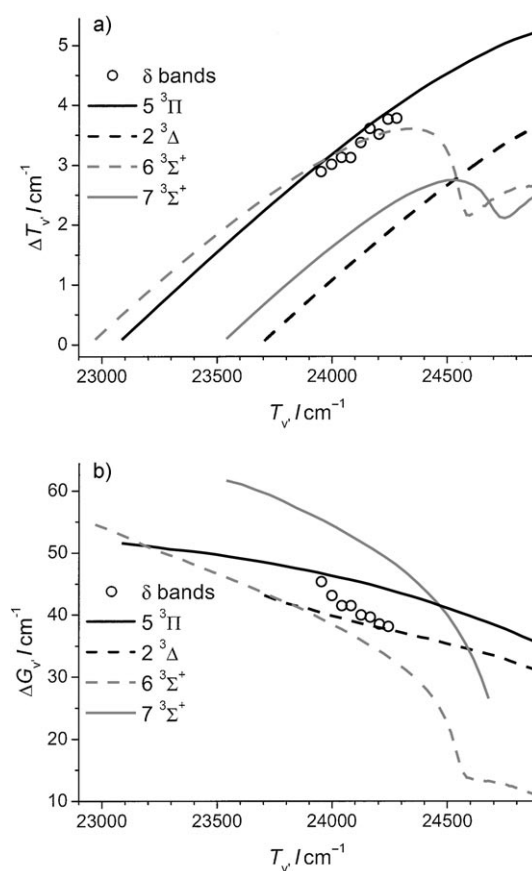


**Figure 8.** a)  $\Delta T_v [= T_v(^{39}\text{K}^{85}\text{Rb}) - T_v(^{39}\text{K}^{87}\text{Rb})]$  and b)  $\Delta G_v$  values of  $\delta$  bands and those theoretically predicted for the  $5^3\Pi$ ,  $2^3\Delta$ ,  $6^3\Sigma^+$ , and  $7^3\Sigma^+$  states. The theoretical values were calculated using the ab initio PECs from ref. [8].



their vibronic structures were clearly resolved in the REMPI spectrum at  $m/z=126$  by isotope shifts. The vibronic structures were revealed by a laser resolution of  $\sim 0.1 \text{ cm}^{-1}$  ( $\Delta\nu_{\text{fwhm}}$ ). The dye laser wavelength was calibrated by Ne and Ar optogalvanic spectra.

## Acknowledgements

This work was supported by NRF of Korea (2009-0071746, 2009-0085319, and 2010-0001484). SL thanks GRRC for financial support.

**Keywords:** alkali metals • excited electronic states • KRb • laser spectroscopy • vibrational spectroscopy

- [1] A. Jraij, A. R. Allouche, S. Magnier, M. Aubert-Frécon, *J. Chem. Phys.* **2009**, *130*, 244307.
- [2] M. Korek, S. Bleik, A. R. Allouche, *J. Chem. Phys.* **2007**, *126*, 124313.
- [3] M. Korek, Y. A. Moghrabi, A. R. Allouche, *J. Chem. Phys.* **2006**, *124*, 094309.
- [4] S. Magnier, M. Aubert-Frécon, A. R. Allouche, *J. Chem. Phys.* **2004**, *121*, 1771.
- [5] H. Fahs, A. R. Allouche, M. Korek, M. Aubert-Frécon, *J. Phys. B* **2002**, *35*, 1501.
- [6] M. Korek, A. R. Allouche, M. Kobeissi, A. Chaalan, M. Dagher, K. Fakherddin, M. Aubert-Frécon, *Chem. Phys.* **2000**, *256*, 1.
- [7] A. R. Allouche, M. Korek, K. Fakherddin, A. Chaalan, M. Dagher, F. Taher, M. Aubert-Frécon, *J. Phys. B* **2000**, *33*, 2307.
- [8] S. Rousseau, A. R. Allouche, M. Aubert-Frécon, *J. Mol. Spectrosc.* **2000**, *203*, 235.
- [9] S. J. Park, S. W. Suh, Y. S. Lee, G.-H. Jeung, *J. Mol. Spectrosc.* **2001**, *207*, 129.
- [10] S. J. Park, Y. J. Choi, Y. S. Lee, G.-H. Jeung, *Chem. Phys.* **2000**, *257*, 135.
- [11] I. S. Lim, W. C. Lee, Y. S. Lee, G.-H. Jeung, *J. Chem. Phys.* **2006**, *124*, 234307.
- [12] S. Magnier, Ph. Millié, O. Dulieu, F. Masnou-Seeuws, *J. Chem. Phys.* **1993**, *98*, 7113.
- [13] B. Kim, K. Yoshihara, S. Lee, *Phys. Rev. Lett.* **1994**, *73*, 424.
- [14] Y. Lee, Y. Yoon, S. J. Baek, D.-L. Joo, J. Ryu, B. Kim, *J. Chem. Phys.* **2000**, *113*, 2116.
- [15] Y. Lee, Y. Yoon, S. Lee, B. Kim, *J. Phys. Chem. A* **2009**, *113*, 12187.
- [16] Y. Lee, Y. Yoon, S. Lee, J. T. Kim, B. Kim, *J. Phys. Chem. A* **2008**, *112*, 7214.
- [17] Y. Lee, S. Lee, B. Kim, *J. Phys. Chem. A* **2008**, *112*, 6893.
- [18] Y. Lee, S. Lee, B. Kim, *J. Phys. Chem. A* **2007**, *111*, 11750.
- [19] Y. Kimura, H. Lefebvre-Brion, S. Kasahara, H. Katô, M. Baba, R. Lefebvre, *J. Chem. Phys.* **2000**, *113*, 8637.
- [20] T. Bergeman, A. J. Kerman, J. Sage, S. Sainis, D. DeMille, *Eur. Phys. J. D* **2004**, *31*, 179.
- [21] T. Bergeman, C. E. Fellows, R. F. Gutterres, C. Amiot, *Phys. Rev. A* **2003**, *67*, 050501(R).
- [22] L. Li, S. Kasahara, Md. H. Kabir, Y. Sahashi, M. Baba, H. Katô, *J. Chem. Phys.* **2001**, *114*, 10805.
- [23] N. Okada, S. Kasahara, T. Ebi, M. Baba, H. Katô, *J. Chem. Phys.* **1996**, *105*, 3458.
- [24] S. Kasahara, C. Fujiwara, N. Okada, H. Katô, M. Baba, *J. Chem. Phys.* **1999**, *111*, 8857.
- [25] G. Herzberg, *Molecular Spectra and Molecular Structure I. Spectra of Diatomic Molecules*, 2nd ed., Krieger, Malabar, FL, **1989**.
- [26] Y. Lee, Y. Yoon, A. Muhammad, J. T. Kim, S. Lee, B. Kim, *J. Phys. Chem. A* **2010**, *114*, 7742.
- [27] Tuning curves of the Nd:YAG pumped laser dyes, <http://www.exciton.com/pdfs/Sirah%20Laser.pdf>.
- [28] C. Amiot, J. Vergès, *J. Chem. Phys.* **2000**, *112*, 7068.
- [29] R. J. Le Roy, *LEVEL 7.7. A Computer Program for Solving the Radial Schrödinger Equation for Bound and Quasibound Levels*, University of Waterloo Chemical Physics Research Report CP-661, University of Waterloo, Ontario, Canada, **2005**.
- [30] H. Lefebvre-Brion, R. W. Field, *The Spectra and Dynamics of Diatomic Molecules*, Elsevier, New York, **2004**.

Received: November 30, 2010

Published online on March 4, 2011